A Preliminary Engineering Design of a "Venetian Blind" Direct Energy Converter for a Fusion Reactor

By William L. Barr, Richard J. Burleigh, Warren L. Dexter, Ralph W. Moir, Richard R. Smith; University of California, Lawrence Livermore Laboratory, Livermore, California 94550

Contact information as of 2009 for Ralph Moir is Vallecitos Molten Salt Research, <RMoir@Pacbell.net>, 607 East Vallecitos Road, Livermore, CA 94550.

This work performed under the auspices of the U.S. Atomic Energy Commission.

Abstract

This is a very preliminary engineering design of a new direct energy conversion device for use in conjunction with a mirror fusion reactor. The device described reclaims the energy lost by the reactor through leakage of charged particles. Energy selection is accomplished through the angular dependence of transmission through a system of ribbon grids resembling a venetian blind. In contrast to previously described converters in which the beam of ions from the reactor is expanded in a flat fan-like expander, the beam in this device is expanded in two directions in a conical expander. Problems of grid construction, radiation damage, grid heating, and vacuum pumping are discussed.

A preliminary cost estimate shows that for a power handled of 1000 MW, the cost for the direct converter is $110 million or $110 per kW of power into the direct converter. The efficiency is estimated to be 59% for a two-state collector and 65% for a four-stage collector. Further development of the basic concept could possibly raise the efficiency to as high as 75%. Optimized designs might increase the power handled by a factor of several without significantly increasing the unit cost, thus greatly lowering the cost/kW.

Introduction

The plasma in a fusion reactor is inevitably lost by leakage. The charged particles emerging from the reactor as leakage consist of electrons, deuterons, tritons, and alphas, all with a wide distribution of energy. It is clearly a good idea to recover this energy as efficiently and inexpensively as possible. A scheme for direct conversion of this leakage into electricity has been suggested.[1,2] That scheme employs a flat, fan-like magnetic expander through which the leakage beam from the reactor is guided.[3,4] It simultaneously reduces the density and converts the random motion to directed motion. The flat beam is then guided into a system of collector electrodes at graded potentials. The current from the collector electrodes is fed back to the reactor ion sources. We will refer to this first scheme as Case I.

The present scheme was first described by Moir and Barr.[5] In this scheme the beam from the reactor is expanded two-dimensionally in a conical magnetic expander, instead of in a fan-like expander. Instead of using a system of collector electrodes at graded potentials, energy selection is accomplished through the angular dependence of ion transmission through a system of ribbon grids resembling a venetian blind. We will refer to the second scheme as Case II.

In this paper we examine some of the practical aspects of this new concept. We will discuss some of the problems involved and some possible solutions We will compare some of the advantages and disadvantages of this concept (Case II) to those of the fan-like converter with grade potentials (Case I).

For purposes of comparison, we will describe one particular arrangement in which the ions pass through only one set of venetian blinds and in which the grids are cooled by radiation. The preliminary cost estimate is based on this case.

We will also discuss arrangements in which the ions pass through more than one set of venetian blinds. Higher direct conversion efficiencies may thus be achieved, but direct cooling of the grids will then be required.

In Case I it was assumed that the power in the direct converter was 1,000 MW and the mean energy of the

positively charged particles was 600 keV. A lower energy would have led to a larger and more costly converter due to the power being space-charge limited. In Case II we again assume 1,000 MW into the converter; however, we have found that the mean energy of the positively charged particles can be much lower (167 keV in our example). We chose a lower energy for Case II because the Deuterium-Tritium reaction rate peaks at lower energies, and space charge can be handled even at these lower energies. The difference in space charge handling between these two cases is discussed in Reference 5. The energy was finally determined by the inefficiency arising from charge exchange as the ions passed through the expander. This loss rapidly decreases with increasing energy and at 167 keV the loss of total efficiency was 1.8%.

In Case I all the leakage power from one end of the reactor is directed into one converter. Indeed, with a fan-like expander it would be rather difficult to do otherwise. In Case II we have shown four separate converters, each with an input of 250 MW. There is nothing magic about the number 4 — this is simply to indicate that Case II lends itself to a multiplicity of smaller units. Figure 1 shows the Case II device superimposed on Case I. One advantage of having a number of separate units is that one unit may be shut down for maintenance while the others are kept running. Disadvantages are the duplication of neutron traps and the necessity of providing means to shut off the plasma at each nozzle.

It should be emphasized that this is a very preliminary engineering design — not by any means a complete engineering design. One of our main purposes is simply to stimulate and thought along these lines.

General Description

The machine consists of the following parts (see Figures 1 through 4):

The Reactor which is the source of the charged particles. Part of the reactor output will be removed as thermal energy and converted to electrical energy in a conventional steam generator plant. The remainder is unavoidable leakage and is diverted into the direct converter.

The Neutron Trap which removes neutrons from the beam and allows the charged particles to pass through.

The Expander in which the beam of charged particles is spread to reduce the particle density and to convert the transverse energy into directed energy.

The Ribbon Grid System which collects the charged particles.

A Thermal Power System to convert the remaining heat energy of the charged particles into useful power.

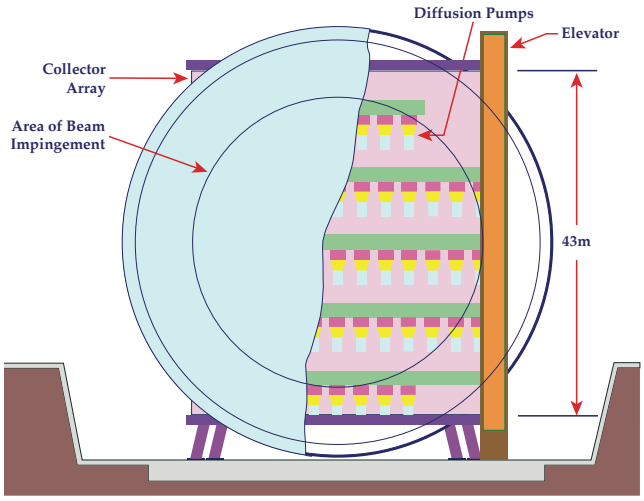

Figure 1 — Plan view showing Venetian Blind converter superimposed on fan type converter. Total beam input to both converters is 1000 MW.

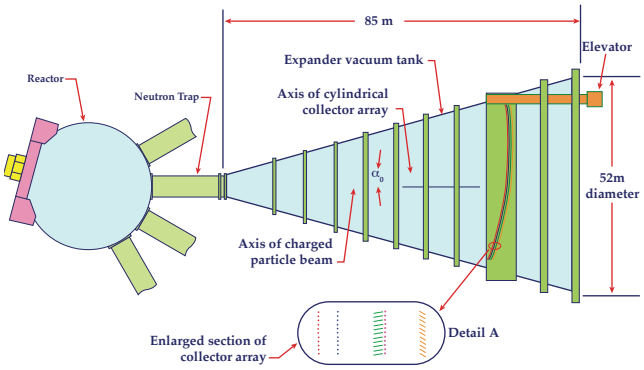

Figure 2 — Plan view of single converter unit. Note angle between axis of charged particle beam and axis of cylindrical collector array.

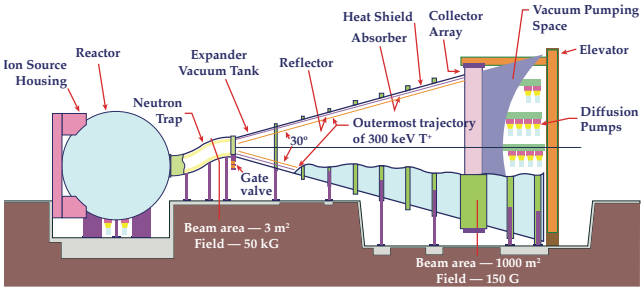

Figure 3 — Elevation view of single converter unit with part of vacuum tank cut away to show internal components.

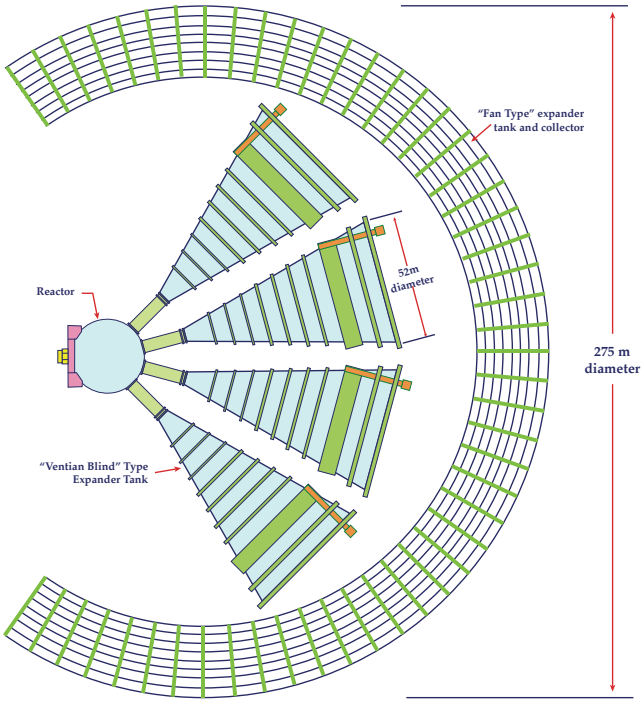

Figure 4 — End view of converter unit with part of vacuum tank removed to show collector array.

A Vacuum Pumping System that removes the large quantities of gas created when the ions are neutralized.

An Electrical System that feeds the current from the ribbon grid system back into the ion sources of the reactor.

The Neutron Trap

It is necessary to remove the neutrons from the beam to prevent activation of the direct converter. To accomplish this, the beam is passed through a reverse bend by means of an appropriate solenoidal magnetic field. The bore of this solenoid is lined with neutron-absorbing shielding. The neutrons being unaffected by the magnetic field, are trapped in the shielding while the charged particles are guided by the magnetic field through the trap. We assume that the magnetic field at the exit from the reactor is 150 kG but drops to 50 kG at the entrance to the neutron trap, and remains constant through the trap. We assume that the cross-sectional area of the beam at 150 kG is 1 m^2 and is 3 m^2 in the trap.

At its entrance end the neutron trap coil must be properly coupled with the fringing field of the reactor, and at its exit end it is really part of the expander coil. The superconducting neutron trap coil is 4.3 m in diameter and 19.5 m long. A gate valve is provided at the exit of the neutron trap so that any converter unit may be isolated. If one unit is closed while the others continue to operate, the selective leakage must be stopped by a magnetic or electrostatic mirror.

The Expander

The beam of charged particles emerging from the neutron trap has a very high power density. This beam must be spread out because of space charge effects and so that the resulting power densities can be handled in a reasonable manner. The expander consists of a large conical vacuum tank with a solenoidal coil attached to the inside surface. The ribbon grid system (described later) is located near the large end of the cone. It appears necessary to carry the solenoidal coil past the grid system to ensure a reasonably uniform field at that cross-section. We have rather arbitrarily selected an area of 1,000 m^2 as the cross-sectional area of the beam at the grid system. This area may be revised after further analysis of the grid heating problem (also discussed later). The field at the grid system is 150 G giving an overall expansion ratio of 1000 to 1 from the reactor to the grids. The field of the expander must be properly coupled with the field of the neutron trap. In fact, the reactor fringing field, the neutron trap field, and the expander field can be considered as one continuous field in which the charged particles flow spirally along the flux lines.

The ampere turns per meter and properties of the magnetic field trajectories were determined by the MAFCO[6] and TIBRO-M[7] computer codes. In most of the expander the field lines look as if they all diverged from a common point about 3.5 m to the left of the junction of the main cone and neutron trap. This means that the field strength decreases inversely as the square of the distance from that point, thus simulating the field of a magnetic monopole. It has been shown that the particle magnetic moment is strictly constant in such a field.[8] A study[9] was made of the trajectories in the magnetic field of the expander. This study confirmed the constancy of magnetic moment.

The trajectory of a 300-keV triton and that of a 14.7-MeV proton will fit inside the structure when they are following the limiting field line. This field line is on the outside of a circle which contains a magnetic flux of 15 Wb and is indicated as "beam" in Figure 3.

The expander windings will be superconducting. Near the apex of the cone, where the fields are high and the windings close together, the windings may be enclosed in a common tank. Further out the turns may be separate elements. A possible cross-section of a superconducting element in its surrounding thermal insulation is described in Reference 2.

A 3200 A superconducting element was chosen for both the neutron trap and the expander. If an excitation time-constant of 1 hour is chosen, then the maximum terminal voltage for the magnet is 500 V. To allow for line drop and regulator margin, the power supply should be rated 563 V and 3200 A (1.8 MW). The magnet power in the expander is smaller than in the neutron trap because

the average field is much less. Again, if we use 3200 A conductor, the maximum magnet terminal voltage is 50 V for an excitation time-constant of 1 hour. Like the neutron trap coil, the power supply should be current regulated and programmable. It should be rated 75 V and 3200 A (240 kW).

The estimated power required to initially excite the neutron trap coil and the expander coil is then 2040 kW. The estimated refrigeration power is 2120 kW. These numbers are for one converter only — for four converters, the corresponding powers are 8160 kW and 8480 kW, respectively.

For reasons which will be discussed later, we propose to use a cylindrical array for the ribbon grid system rather than the more nearly ideal doubly curved surface (approximately spherical). To minimize the error thus introduced, the cone should be narrow and therefore long; however, to minimize the cost of the tank, the cone should be short. We have rather arbitrarily selected a cone angle of 30° for the illustration.

The above considerations lead to a tank length of 85 m and an end diameter of 52 m. This is, needless to say, a tremendously large vacuum tank! However, this is not a huge extrapolation of a vacuum tank built at Lawrence Livermore Laboratory in the early 1950s. That tank was cylindrical with inwardly dished ends and was 18 m in diameter and 26.5 m long. The cylindrical portion was reinforced with 14 T-section rings 84 cm in radial depth and had 15 cm I-beams 91 cm apart around the circumference, extended between the rings, to act as longitudinal stiffeners. The wall thickness of the cylindrical section was 1.27 cm. The spherical radius of the dished ends was 14.6 m and the wall thickness was 0.95 cm. We quote these numbers simply to give an idea of the dimensions involved.

Preliminary crude design numbers based on a working stress of 20,000 psi for the tank in our present case are as follows. With a spherical radius of the dished end of 34 m, and using the standard stress formula ($\sigma = PR/2t$), the wall thickness is 1.27 cm. With a reinforcing ring every 6 m along the length, and with the longitudinal stiffeners spaced 1.2 m apart around the circumference, the wall thickness of the conical section is 2.5 cm. The stiffener ring at the large end might have a radial depth of 1.8 m, a web thickness of 2.5 cm, a flange width of 61 cm, and a flange thickness of 5 cm. The dimensions of the stiffener rings become progressively smaller toward the small end of the cone. These dimensions are simply presented as working numbers, not as an optimized design. The weight of one tank is about 3×10^6 kg, or 1.1×10^7 kg for four tanks. This compares with the total weight of 5.3×10^7 kg for the expander tank and the collector tank of Case I.

The Ribbon Grid System

At the heart of this machine is the ribbon grid system for collecting the charged particles. As shown in Figure 5, the plane of the grid system is at a small angle relative to the incoming beam of charged particles. The particles first see a wire grid at zero potential, then a second wire grid at negative potential. The function of this pair of grids is to reflect the electrons and allow the ions to continue through these grids. The ions next see a grid of venetian-blind-like ribbons which are at a positive potential. Beyond this is another ribbon grid at a positive potential about twice the potential of the first ribbon grid. As the ions approach at an angle to the uniform electrical field produced by this pair of ribbon grids, their trajectories are parabolic. As the incoming ions are aligned with the first set of ribbons, the grid appears relatively transparent. After the ions have lost their forward motion they turn around and then see a relatively opaque grid. Some less energetic ions will strike the first ribbon grid on their passage through. Some more energetic ions will not turn around between the two ribbon grids but will strike the second grid. It can be seen, then, that this grid system acts as an ion trap. A third wire grid is placed in the shadow of the first ribbon grid to suppress the secondary electrons. As far as functioning as part of the ion trap, the second ribbon grid could be simply a continuous flat plane. However, as the beam stops and delivers its charge, it becomes a neutral gas. By making the plane into a ribbon grid, it is opaque to ions but transparent to this gas, allowing the gas to be pumped out of the system.

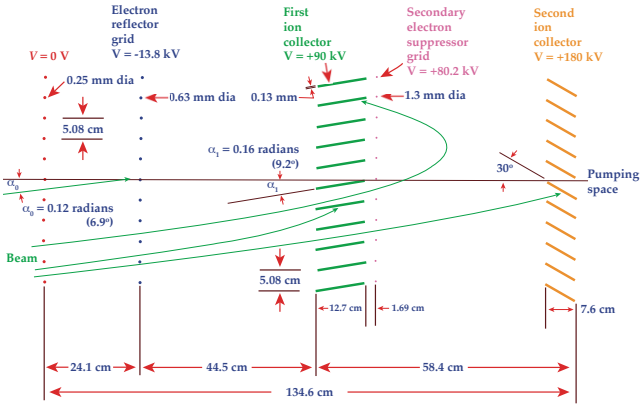

Figure 5 — Collector and grid array. The pair of wire grids at the left reflect the electrons and allow ions to pass on through the venetian blind collector. The venetian blind appears transparent to the incoming ions but opaque to the ions reflected by the second collector.

Plots of the potentials surrounding the various elements of the grid are shown in Figure 6. These potential plots were made by the technique of painting conducting boundaries on resistance paper and plotting equipotential lines. From these plots we were able to determine the potential on the suppressor grid required to return

all secondary electrons to the collector, to determine the electric field on the grid wires, and to estimate the defocussing due to the fringing fields around electrodes.

The charged particles are not, of course, traveling along parallel lines but appear to radiate from a point at the apex of the expander. This means that the grid system should not be simply a flat plane but should be a three-dimensional curved surface, such that all particles approach it at the same angle. For small cone angles this surface can be approximated by a sphere, the axis of which is slightly inclined to the axis of the cone. It is difficult, however, to construct a grid of wires and ribbons on a spherical surface.

We therefore locate the grids on cylindrical surfaces. If the cone angle is small the correct cylindrical surface can be approximated by a circular cylinder, the axis of which is slightly inclined to the axis of the cone as shown in Figure 2. To eliminate sag in the wires and ribbons due to gravity, we arranged them vertically.

If we consider a particle approaching the grid on the axis of the cone, it will approach the central ribbon at the correct angle of attack. If we consider another particle approaching the same central ribbon at, say, the lower end of the ribbon, the angle of attack will not be quite correct.

This error is, however, quite small. Furthermore, as shown in Reference 5, the efficiency is relatively insensitive to small changes in entrance angle.

One of the problems connected with direct converters is ion bombardment damage resulting in the deterioration of the surfaces on which ions are collected.[10] The damage is of two types, sputtering and surface spalling, and is caused by buildup of helium and hydrogen. Since sputtering loss rates are extremely low, this appears benign.

However recent experiments have been performed with 300-keV helium ions impinging on stainless steel at various temperatures. For doses of ~10^{18} ions/cm^2 the surfaces become flaked except at high temperatures (700°C). It is possible that flake formation could lead to voltage holding problems by greatly magnifying the electric field at the edges of the flakes.[11]

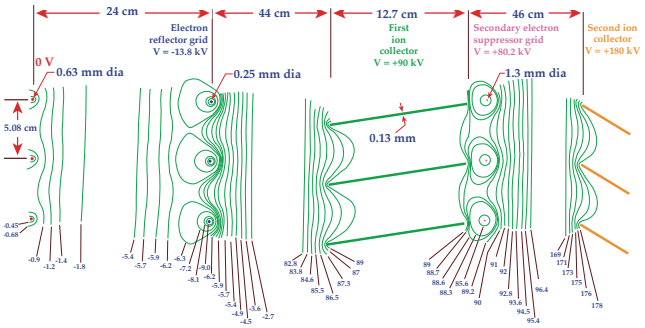

Figure 6 — Equipotentials for two-collector converter. Note that (1) all potentials are kV, (2) unless otherwise noted, all potentials are positive, (3) green lines between first ion collector and second ion collector indicate potentials below 90 kV, and (4) green lines between zero-volt grid and first ion collector indicate potentials of zero volts or less.

One solution to this damage problem would be to replace the collectors every 40 hours as discussed under "Radiative Heat Transfer." Another solution[10] would be to coat the surface with a material which would sputter away at the same rate as flakes occur. It might be possible to run the collectors quite hot or to periodically heat their surfaces to remove any bubbles and relieve the helium pressure. The damage problem certainly needs more study and experimental tests. At present this damage phenomenon is not completely understood, but we think that it may make the replacement of ion collectors a necessity.

The present concept appears to lend itself to the replacement of the ion collectors with minimum expense and without shutting down the machine. In Figure 7 we have shown schematically how the ribbon may be fed into and out of the vacuum tank. This might be done slowly and continuously or on a batch schedule. We show the ribbons passing through a labyrinth seal in which successive stages are pumped to minimize the leakage. Brushes are provided to take off the current before the ribbon enters the seal. The current on any one ribbon is only a few amperes. Drives are provided on the reels to apply the proper tension. To keep the ribbons straight and true, low interception spacers can be used.

Or it may be necessary to apply considerable tension (probably sufficient to exceed the elastic limit when hot). Another possibility might be to make the ribbons from graphite cloth with tungsten wire supports. The whole seal and reel assembly is separated from the tank by an insulator of glass-reinforced epoxy.

The ribbons shown in the illustration are 12.7 cm wide and 5.08 cm apart. Other dimensions could be used, keeping the whole array of wires and ribbons geometrically similar. To provide the greatest transparency to the

incoming ions, the ribbons should be thin as possible — 0.13 mm seems reasonable.

The ribbons are cooled by radiation (see "Radiative Heat Transfer") to a water-cooled linear to be described in a later section. The ribbons will run very hot, in the neighborhood of 1100°C. The ribbons will be made of a refractory material such as niobium, the melting point of which is 2468°C. The cost estimate is based on the use of this material. Other materials which might be considered are titanium, molybdenum, tantalum, tungsten, and woven graphite filaments. Table I shows the comparison of the melting points and cost of these materials.

The Grounded Grid

An electron current equal in magnitude to the ion current must also escape from the reactor so that charge neutrality is maintained. We assume that most of this electron current will escape through the weaker magnetic mirrors at the entrances and accompany the ions down an expander. The negative grid will reflect the electrons before they reach the positive ion collectors. The electrons will be reflected back and forth along the expander between the negative grid and the strong magnetic mirror at the far side of the reactor.

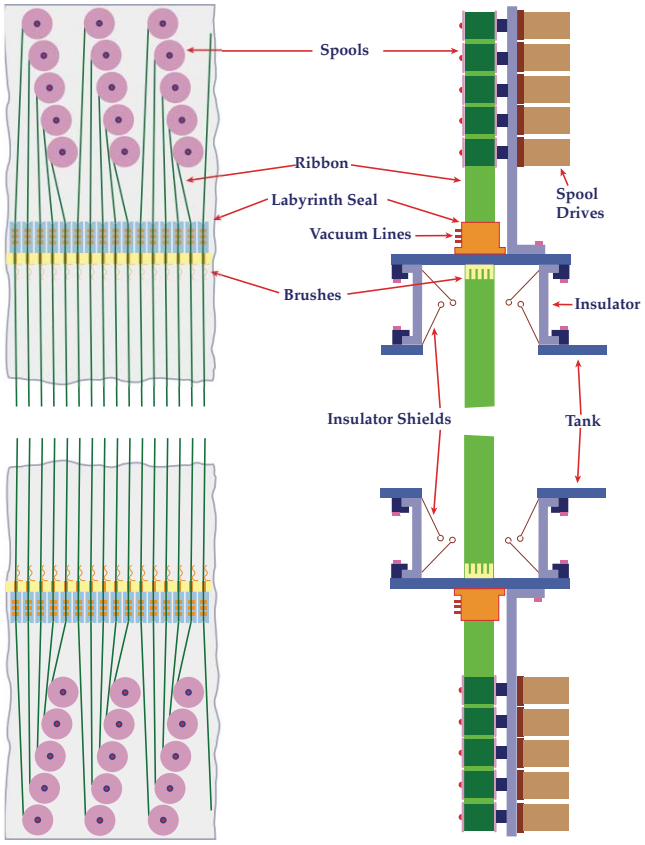

Figure 7 — Termination of venetian blind ribbons showing vacuum seals, brushes to remove current, and spools and drives. Ribbons may be replaced without shutting down the converter.

Table I — Melting point and costs for various ribbon materials

Material	Melting Point °C	Dollars/kg	Total kgs for 4 units	Total Cost
Titanium	1668	31	23,000	$714K
Molybdenum	2610	65	45,000	$3,000K
Tantalum	2996	75	8,000	$6,300K
Tungsten	3410	180	90,000	$16,000K
Woven Graphite	3727	65	9,000	$600K
Niobium	2468	40	42,000	$1,600K
Stainless Steel	1500	2.8	40.000	$106K

Weight based on 0.13 mm thick, 12.7 cm wide except woven graphite which is 0.63 mm thick.

Their ultimate fate probably is collection on a wire in the grounded grid through which they must pass after each reflection. Some electrons will be scattered into a loss cone and escape through a strong magnetic mirror to a wall. However, most of the electron current will probably be carried by the wires of the grounded first grid. It is therefore necessary that those grid wires be capable of carrying that current.

The wires will be hot because of resistive heating due to the electron current and due to bombardment by ions. Electron energy is assumed to be negligible.

We calculate the necessary size of tungsten wires if their temperature is to remain low enough to prevent thermionic emission while being radiatively cooled. Consider the longest wire, which spans the center of the grid, and assume the wires are spaced 5 cm apart. That wire must carry 2.7 A for an average distance of 13.4 m. It receives 25 W/cm^2 of beam on its projected area, and it can radiate to cool walls and a lesser amount to the hot ribbons. By balancing the heat radiated with the total rate of heating, We find that a 0.5 mm diameter wire (for 1% opacity) would run at 1520°C. If the spacing is increased to 7.5 em, the central wires each will carry 4 A and a 0.75 mm wire (1% opacity) would run at 1500°C. Increasing the size of the wire beyond this doesn't change the temperature because the heating is due mostly to beam interception which is proportional to surface area as is the radiative cooling.

At these temperatures, the thermionic emission from tungsten is about 1 x 10^{-5} A/cm^2, or 6 mA per wire. This emission current is negligible — especially from the grounded grid, Since the negative grid prevents electron current from going to the positive collectors. The negative grid will run at nearly the same temperature so that it too must be made of tungsten and will emit about 6 mA per wire if 0.5 mm wires are used. About half of this emission current will go to the collectors. resulting in about 0.1% loss in efficiency.

Thermal Power System

Obviously, not all of the ion energy is converted into electricity. The energy of most of the ions will not match the potential of either of the collector grids, and this mismatch results in heating. Calculations indicate that the direct conversion efficiency may be about 60%; in this case 40% of the energy then goes into heating the ribbons. As we are assuming an input of 250 MW into each of the four units, 100 MW goes into heat. We can further assume the 100 MW is evenly divided between the two ribbon grids. We also assume that the peak beam load on the surface of the grids is twice the average load.

We propose to transfer the heat from the ribbons, by radiation, to a water-cooled liner. As shown in Figure 3, this water cooled liner or absorber will line a portion of the conical part of the tank and also will extend over the entire back of the tank. That portion of the conical tank which is not lined with absorber will be lined with a reflector. A multilayered heat shield of polished metal is placed between the tank and the absorber. At the back end, baffles are provided in the absorber and heat shield for vacuum pumping. Steam will be produced in the pipes of the absorber. The steam will be returned to the main steam generator plant powered by the reactor. To ensure good thermal efficiency in the generator plant, we propose to run the liner at a temperature of about 540°C.

Calculations for the temperatures of the ribbons are shown under "Radiative Heat Transfer".

Vacuum Pumping Requirement

Each 250 MW unit will carry 1500 A total current if the mean ion energy is 167 keV. Integration of the distributions of current shown in Figure 8 gives the electrical current carried by each of the species as:

$I(D^+) = 915$ A

$I(T^+) = 570$ A

$I(He^{++}) = 26$ A

The distributions at injection energies other than 100 keV were scaled from the results of that one calculation. A check on the consistency of the data shown in the figure is obtained from the definition of Q for the reactor:

$$[I(D^+)W(D^+) + I(T^+)W(T^+)]Q = (1/2)I(He^{++})W(\text{fusion})$$

Here, the injection energy is $W(D^+) = W(T^+) = 150$ keV, $Q = 1.357$, and $W(\text{fusion}) = 22.4$ MeV. This method predicts $I(He^{++}) = 27$ A, in reasonable agreement with the 26 A found by numerical integration of the curves in the figure.

The total ion current is 9.3 x 10^{21}/sec, so that the vacuum pumps must handle 5 x 10^{21} molecules/sec, or 130 torr-liters/sec. This will probably be the main source of gas that must be removed by the pumps. The pumps must have enough pumping speed to maintain the pressure below a level set by the maximum allowable rate of power loss due to charge exchange.

Any ion that undergoes charge exchange with a gas atom will proceed as a fast neutral. If the charge exchange occurs anywhere in the last 70 m of the expander, the resulting neutral will strike a hot surface from which its energy will be recovered in the thermal cycle. Since

thermal efficiency is about 40%, while that of the direct converter is 60%, the actual energy loss due to a charge exchange event is only 36% (thermal only vs direct recovery plus thermal). This loss of power can be kept low by keeping the pressure low — but, at the cost (in money and power) of more pumping speed. There is, therefore, an optimum pressure for the expander and collector system.

As an example, we calculate the pressure where 3% of the ions undergo charge exchange. This results in a 1.08% loss of power (1.8% less from the direct converter, 0.72% more from the thermal converter). The cross-section for charge exchange of D^+ on D_2, when averaged over the energy distribution $W\,dI/dW$ obtained from Figure 8, is $\sigma = 0.8 \times 10^{-16}$ cm² per neutral molecule. Therefore, 3% of the D+ ions are lost when:

$$0.03 = n_{\sim o} L \sigma$$

where L = 80 m is the length of the expander, and $n_{\sim o}$ is the molecular density. This gives $n_{\sim o} = 4.7 \times 10^{10}$/cm³, or $p = 4.6 \times 10^{-6}$ torr if the temperature of the gas is 540°C. The required pumping speed is then 130 torr-liter/ sec at 4.6×10^{-6} torr, or $S = 2.8 \times 10^{7}$ liters/sec.

Commercial 122 cm oil diffusion pumps are claimed to pump hydrogen and helium at about $S_p = 1.4 \times 10^5$ liters/sec per pump. Therefore, 200 such pumps will be required per expander cone. In actual operation, S_p may be less than this so that either more pumps may be required or operation at higher ion energy may be necessary. Since the installed cost of these pumps is about $15K each, the total cost of the pumps is about $3M per cone, or $12 per kW handled. If power consumption is 36 kW per pump, the pumps will consume 7MW per cone. However, this heating power might be nearly free if the exhaust from the turbines is used to heat the pumps.

Also, since there are other ways (e.g., by getter pumping or by condensation pumping) to pump D_2 and T_2 it may only be necessary to provide enough diffusion pumps to handle the He. The flux of He is only 0.9% of the total particle flux, so four pumps would be adequate to pump just the helium.

The pumping problem becomes less severe when the mean energy of the ions is raised. For one thing, as the energy is raised the current can be reduced for a given amount of beam power. Another thing is that the cross-sections for charge exchange decrease with increasing energy. Figure 9 shows the variation with ion energy of four important parameters - Q, σ, p, and N. Q is the gas load (torr-liters/sec) due to the beam current for 250 MW into an expander cone. The average cross-section, σ, for charge exchange of D+ in D_2 was calculated using the energy distribution shown in Figure 8 after simply rescaling all energies in proportion to injection energy.

The pressure, p is that level at which 3% of the ions undergo charge exchange with background gas in the 80 m expander. A gas temperature of 540°C is assumed. Finally, N is the number of pumps required if each pump has a pumping speed $S_p = 1.4 \times 10^5$ liters/sec (manufactures specifications for H_2 in a 122 cm oil diffusion pump). Further work is needed on providing room for more pumps since we require 200 pumps whereas Figure 4 only shows 55 pumps. Although adequate conductance to the pumps must be kept in mind, this problem doesn't appear too serious.

Electrical System

To initiate the collection process, the potentials of the grids and "Venetian Blinds" must be accurately established as shown in Figure 10. Once the potentials are established and the collection process begins, the electrical energy recovered should be used as efficiently as possible. A natural use of the power is for the fusion reactor ion sources. There is a lower voltage limit at which injection becomes inefficient. We have arbitrarily chosen to convert the 90-kV venetian blind power to 120-kV standard power line potentials by rectifier-inverters which are described elsewhere.[2] This power can be transformed and rectified for ion-sources or can be used for other purposes. The power from the 180-kV venetian blind is used directly by the ion sources and is fed by means of a suitable high voltage cable.

The first grid in the system is at zero potential and is grounded to the expander tank.

The potential on the second grid is established at negative 13.8 kV by means of a regulated power supply. The current of this supply is 50 A and is required because approximately 1% of the total current of the direct converter beam impinges on the grid. Also, about 3% of the ions will undergo charge exchange with gas in the expander. About one-half of the resulting cold ions will ultimately be collected on the negative grid. The other half will go to the grounded grid.

The positive 90-kV potential on the first venetian blind electrode is supplied by inverter-rectifiers. When operated in the rectification mode, these inverter-rectifiers supply the voltage; as the power flow reverses, the inverter operation begins and power is supplied from the collectors to a common power line through an isolating transformer. The phasing of the inverters and rectifiers is controlled by an electronic regulator system that maintains the electrode potential called for by the regulator reference.

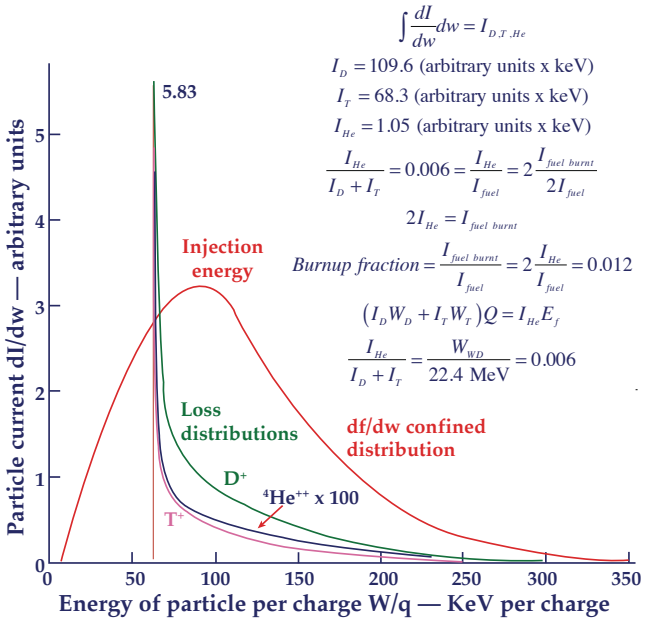

Figure 8 — Energy distribution of particles leaking from the plasma into the direct converter for 100 keV injection. The mirror ratio was 10, Q = 1.36 for 100 keV injection. Note that although the He ions are born with 3.52 MeV their mean escaping energy is only about twice that of the D^+ or T^+ and is a factor 100 down in intensity. The case treated in the text in scaled from this.

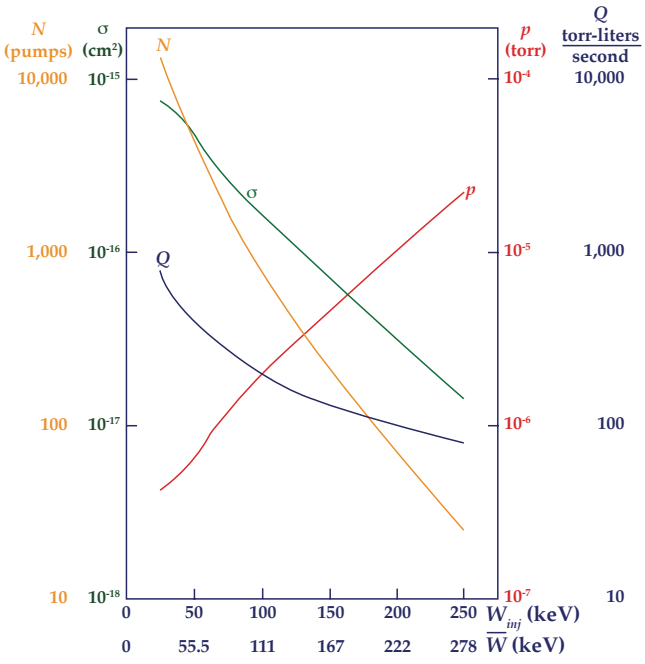

Figure 9 — Plots of the parameters that determine the vacuum pumping requirements: Q is the gas throughout due to the ion beam, a is the cross-section for charge e~change of D^+ with D_2, *p* is the pressure at which 3% of the ions undergo charge exchange, and *N* is the number of 1.4 x 10^5 liters/sec pumps required.

The purpose of the third grid is to suppress secondary electrons that are formed on the venetian blind electrodes. A potential of positive 80.2 kV relative to ground (or negative 9.8 kV with respect to the first venetian blind electrode) is established by means of a regulated power supply rated at 12.5 A. The grids and venetian blinds are coated with emission suppression materials such as carbides, silicides, or borides (as is also done in high power vacuum tubes).[12] When estimating the loss due to secondary electrons, however, we take the emission coefficient equal to 3.

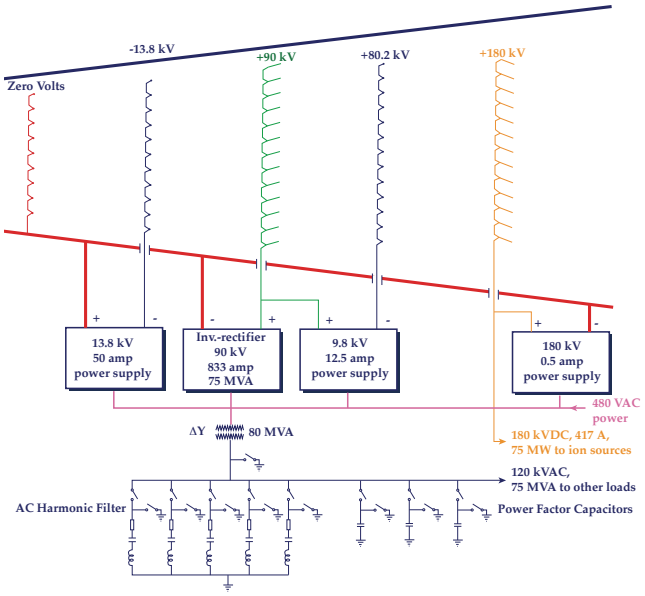

Figure 10 — Electrical schematic of the direct converter. The 90-kV venetian blind power is converted to AC by solid-state inverters and transformed to 120 kV.

The second venetian blind electrodes are established at positive 180 kV by means of a regulated power supply. When the collection process starts, the power goes directly to the ion source loads and the power supply floats, drawing no current.

Semiconductor inverters and phase controlled silicon rectifiers produce harmonics in the power line. The harmonics can be reduced by means of filters such as those used in the power industry. Power-factor capacitors are also included so that the inverters will feed an optimum load.

Electric Fields at Grid Wires

Electrical breakdown is most likely to originate at that point on a negative surface (relative to its surroundings) where the electric field is strongest. In Figure 6 it can be seen that the strongest field at a negative surface exists at the wires in the negative grid and in the suppressor grid.

On the side of the negative grid wires facing the +90 kV ribbons, the field strength is 66 kV/cm for the geometry shown in Figure 6. It can be shown that this maximum field varies almost linearly with the transmittance of the

grid divided by the grid-to-ribbons spacing. The grid shown in the figure is 1.25% opaque. It is not desirable to increase the grid interception much beyond this. However, the grid-to-ribbon spacing can be increased from 44.5 cm to 125 cm before the collected current becomes space-charge limited (see Space Charge Considerations later in this paper). Increasing the spacing can therefore reduce the maximum field to 24 kV/cm. This would be a modest gradient normally. However, here the wires are being sputtered and heated by ion bombardment. Thermionic emission current is about 10 uA/cm^2 if pure tungsten is used. Voltage holding under these conditions may be a problem and needs further study. However, if this is a problem, it is possible to increase the edge radius of the elements to reduce the gradient magnification. (In the Case I study, 100 kV/cm was accepted as the maximum gradient.)[2]

Efficiency

In talking about the efficiency of the direct converter we are only considering the fraction of power carried by the charged particles leaking out of the reactor which is converted directly to electricity. We denote this direct conversion efficiency as η_{DC}.

Most of the energy not directly converted (1 - η_{DC}) enters a conventional thermal conversion system of efficiency η_{TH}. The fraction of the charged particle power ending up as electricity then is approximately

$$\eta_{DC} + (1 - \eta_{DC})\,\eta_{TH}$$

As an example, if both η_{DC} and η_{TH} are 50% then the combined conversion efficiency is 75%. In this mode of operation the direct converter is a topping cycle and the thermal converter is a bottoming cycle.

Figure II is the flow diagram for the power carried by charged particles. The expected efficiency of each process is shown for a two-stage collector system with those for a four-stage system shown in parentheses. The various efficiencies shown in the figure were determined as follows:

Coupling to the Reactor

We employ the principle that the particles will selectively leak out the end regions where the mirror magnetic field is weakest due to small angle scattering into the loss cone. Recent calculations by G.A. Carlson[13] indicate that as little as 90% of the leakage might be into the direct converter and the rest would go elsewhere ending up as heat. It may be possible however to direct virtually 100% of the leakage into the direct converter by electrostatic stoppering[14] of most of the exciting field lines. Due to uncertainties in the calculation and in the concept of electrostatic stoppering, we somewhat arbitrarily assume 97% of the leakage is directed into the converter.

Charge Exchange Loss

The ions traveling down the expander have a chance of being converted to neutrals by charge exchange on the background gas. For a D_2 pressure of 5 x 10^{-6} torr (as discussed in the section on pumping), the fraction of the beam that avoids charge exchange is 97% for an injection energy into the plasma of 150 keV.

Ion Collection

The various losses encountered in the collection process (see Table II) include:

a. **Ideal Efficiency** - If each ion was collected on the highest potential electrode which it could energetically reach then the loss due to impacting the electrode with excess energy would be minimized. This efficiency has been calculated for the D^+ ion energy distribution of Figure 8 and is given in Table II.

b. **Interception on Non-ideal Collectors** Some ions which have enough energy to be collected on a given collector are actually collected on other lower-potential or grounded electrodes or even on a negative electrode. We have estimated this loss based on the accelerated Maxwellian distribution discussed in Reference 5, where the ideal efficiency was 0.54, 0.71, 0.79 and 0.83 for 1, 2, 3, and 4 collectors, respectively.

c. **Injection Angle** α_o - The optimum injection angles were reported in Reference 5. The perpendicular energy is proportional to cos2 α_o and is recovered only as heat.

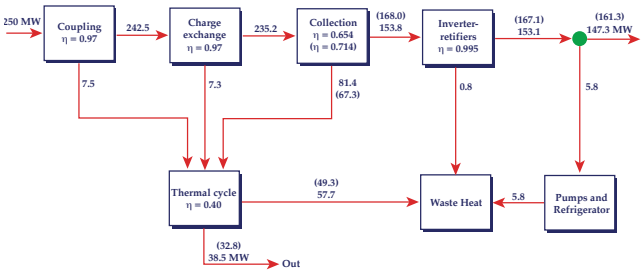

Figure 11 — Power flow diagram showing the flow of 250 MW of ion beam power through the various processes involved in direct conversion. Efficiencies, η, and power are shown for a two-stage system, with the numbers for a four-stage system in parentheses.

Table II — Efficiency losses in the collection process

	Number of Collectors			
	1	**2**	**3**	**4**
a. Ideal collection	-0.43	-0.26	-0.19	-0.15
b. Interception by non-ideal electrodes	-0.01	-0.03	-0.05	-0.06
c. Injection angle,	0	-0.014	-0.023	-0.026
d. Angular spread	-0.001	-0.012	-0.016	-0.018
e. Defocussing	-0.001	-0.004	-0.005	-0.005
f. Parallel motion	-0.015	-0.015	-0.015	-0.015
g. Secondary electrons	-0.006	-0.007	-0.008	-0.008
h. Space charge	-0.002	-0.004	-0.004	-0.004
Collection losses	-0.465	-0.346	-0.311	-0.286
Collection efficiency	0.535	0.654	0.689	0.714

d. **Loss Due to Angular Spread** — The angular spread is related to the transverse energy which in turn is related to the magnetic field expansion ratio. For an expansion of 1000, the angular spread is ±0.03 radians. The inefficiency due to this angular spread has been calculated by the computer code called LOUVER.[5] The code calculates the angle and dimensions of the several electrodes which gives the optimum efficiency for the best entrance angle, α_o. Then the code calculates the efficiency for the entrance angle $\alpha_o \pm 0.03$. The loss shown in the table is the difference between the efficiency for α_o and the efficiency obtained by a simple average at $\alpha_o - 0.03$, α_o, and $\alpha_o + 0.03$.

e. **Defocussing by Fringing Electric Fields** — The beam of ions will be defocussed somewhat by the nonuniform electric fields near the various grids and ribbons. In passing close to a grid wire, an ion trajectory is deflected through an angle $\Delta\theta$ radians:

$$\Delta\theta = \frac{\pi q c}{2W} \quad (1)$$

Here q is the charge on the ion, W is its kinetic energy, and c is a constant given by:

$$c = \frac{V_g - V_1}{\ln\left(r_g / r_1\right)} \quad (2)$$

where V_g and r_g are the potential and radius of the grid wire, respectively, and V_1 is the potential at radius r_1. If r_1 is the largest radius of any equipotential surface that is roughly circular, then all trajectories with the same energy will be deflected through the same angle $\Delta\theta$ if they pass within a distance r_1 of a wire.

In Figure 6 it can be seen that $r_1 \approx 1.8$ cm near a wire in the negative grid. Therefore, about 35% of the beam (D^+ with 180 keV mean energy near the grid) is deflected through $\Delta\theta = +0.70^\circ$ and another 35% is deflected through intermediate angles. The negative grid therefore has the effect of increasing the divergence of the beam from $\pm 1.7^\circ$ to $\pm 2.4^\circ$.

At the 90 kV collector ribbons, the mean kinetic energy is 74 keV. An analysis of the equipotential plots in Figure 6 shows that the deflection, when passing within 1.0 cm of a ribbon, is about 0.5° away from the ribbon at the

leading edge plus another 0.5° in the same direction at the trailing edge.

The combined effect of the deflection at the negative grid and at the leading edge of a ribbon is to increase the fraction of the beam intercepted by the ribbon on the forward pass. The increase is about the same as if the initial divergence of the beam were increased from ±1.7° to ±2.2°. In Reference 5 it is shown that this results in a decrease in efficiency of the device by less than 1%. This is a small effect, and it can be made smaller by properly positioning the grid wires. If the wires are located on streamlines passing midway between ribbons, then only those ions with energies close to the ribbon potential can be deflected into a ribbon. But, it is in fact desirable to have those ions collected on the ribbons whether on the forward or return pass. It appears then that defocussing by fringing fields can have a negligible effect on the overall efficiency of the device. In the table, the loss due to defocussing by fringing fields is taken from item "d" above and adjusted in the ratio 0.5°/1.7°.

f. **Loss Due to Motion Parallel to the Ribbons, W_1.** Those ions entering near the top of the cone would have some energy perpendicular to the applied field. This energy is not directly recoverable. The worst case is the ion entering at the top of the 30° cone. The loss is $\sin^2 15°$ or 0.067. When averaged over the entire cone, this is estimated to be 1.5%. This loss could be eliminated by curving the grids onto a spherical surface.

g. **Loss Due to Secondary Electrons**. There are two losses due to secondary electrons. The first loss arises from electrons produced by ion impact on the negative electron reflector grid. These electrons carry away eV_g of energy. The second loss arises from ions hitting the back of the secondary electron suppressor grid making secondary electrons which then are accelerated to the next collector. These losses have been estimated in Reference 5 for a secondary emission coefficient of 3.0.

h. **Finite Space Charge** — Preliminary estimates indicate the effect of space charge in the vicinity of electrodes should cause defocussing comparable to item "e" above.

Loss in the Inverter

This device can be 98.5% efficient;[2] however, we would only invert, step up, and rectify the current collected on the lower voltage electrodes (the 90 kV electrode for the two-collector case) because we assume 90 keV is too low an energy to be efficiently reinjected.

Power for Pumps

If we assume 200 pumps are used, each consuming 36 kW of thermal power, then compared to the incident 250 MW of power the pumps will consume 3% of this power. We will further drop this loss by a factor of two due to the use of surface pumping to cut down the number of pumps, more efficient pumps, or the use of waste heat.

Refrigerator for the Magnets

If the refrigerator for the magnets is assumed to be the same size as for that of Reference 2 then it will consume 2120 KW of power for each 250 MW unit, giving a loss of 0.8%.

Other Effects

Studies of back streaming electrons, and X-ray related losses such as carried out by Julian and others[15] should be done. Also, techniques for improving the efficiency should be explored. If the fraction of ions not leaking into the direct converter could be halved, the efficiency could easily increase by 0.5% or so. If losses associated with background gas were eliminated, a 2% gain would result. If all the losses in Table II could be halved except the ideal collection loss, a 7% gain could be expected. These increases total 10%. The four-collector efficiency of 65% (see Figure 11) could be described as a "present day" estimate. A fully optimized and refined converter of this type might achieve 10% higher or 75%.

Space Charge Considerations

Space charge of the ions will modify the applied potential. Because the collector structures are essentially plane surfaces, the modified potential will simply distort the otherwise parabolic trajectories between collector structures. The ions will still be collected at the same potential (i.e., the same amount of energy will be recovered) if the space charge is not allowed to reverse the direction of the electric field anywhere. The situation is similar to space charge considerations in a plane diode, except that here there is a distribution of energy and there are reflections. Just as for a plane diode, space charge sets a limit on the current density, which is proportional to the three-halves power of the potential difference divided by the square of the distance between electrodes.

The proportionality constant was calculated for the energy distribution given in Figure 8 using the computer code SPACH.[16]

The energy distribution in turn was calculated with a Fokker-Planck code,[17] recently modified,[18] to calculate

the energy distribution of ions leaking from the reactor into the direct converter. Using the energy distribution in Figure 8 for D^+, we calculated the optimum collector potentials which would give the greatest efficiency with a code called COP (Collector Optimization Program).[19] For two collectors, the potentials were 90 kV and 180 kV. Using the space-charge code SPACH, we found a two-collector system handling 250 MW can have spacings up to 125 cm and 136 cm between the negative grid and the first collector and between the first and second collectors, respectively. A four-collector system with optimum collector potentials of 94.4, 132, 180, and 243 kV can have spacings up to 125, 78, 111, and 176 cm between successive electrodes.

These maximum spacings determine the maximum separation between the ribbons in the collectors in order that the equipotential surfaces be reasonably flat. Irregularities in the equipotential surfaces would produce defocussing of the ion beam as discussed in the section on efficiency. For a four collector system then, the separation H < 19 cm and for not more than 4% interception on the leading edges, the thickness d < 0.8 cm. These dimensions are important because a four collector system cannot be radiatively cooled. It may be desirable to flow some fluid through tubes in the ribbons.

Radiative Heat Transfer

One of the most important problems that must be solved to give the direct converter practical merit is the problem of heat transfer from the collectors. Radiative heat transfer from hot collectors to cooler walls is a possibility which could also provide a solution to the potential problem of spalling due to bombardment by He ions.

Because it could possibly solve two problems at once, we investigated radiation heat transfer. Since both collectors will be hot, radiative transfer will occur predominantly in the direction away from the other collector. The leading edges of the ribbons in the first collector structure "see" a much larger area of cooler surface than the trailing edges. The heat flux to the ribbons due to ion bombardment is nearly uniform over the surface area of the ribbons. This is because the ribbons do not present a completely opaque structure, on either the forward or the reflected path, to any except a very small class of ions, and that class of ions which strike primarily the trailing edges is the class which is collected most efficiently. These ions, therefore, produce the least amount of heat. Thus, the temperature gradient is due almost entirely to the variation in the view factor for radiation from different parts of a ribbon. The ribbons are so thin that conduction across a ribbon doesn't affect the temperature gradient, but radiative transfer from hot trailing half of one to cooler leading half of another ribbon does affect the gradient.

A preliminary radiative cooling analysis was. made by R.W. Werner.[20] Following his approach, view factors were calculated[21] for the exchange of radiation between each pair of surfaces as indicated schematically in Figure 12. Both sides of the ribbons are included. Transmission through the hot rear collector to surfaces at sink temperature T_3 is included in the view factors. Temperature T_3 was taken to be 540°C for good efficiency of the thermal cycle. The emissivity of the ribbons was assumed to be $\varepsilon = 0.3$, which is the value expected if stainless steel is used in this hydrogen atmosphere. Emissivity of the walls was taken to be unity. The effective emissivity $\mathcal{F}_{ij}$ for the exchange of radiation between two surfaces is given by:

$$\frac{1}{\mathcal{F}_{ij}} = \frac{1}{F_{ij}} + \frac{1-\varepsilon_i}{\varepsilon_i} + \frac{A_i}{A_j}\frac{1-\varepsilon_j}{\varepsilon_j} \quad (3)$$

Here A_i and A_j are the areas and F_{ij} is the view factor between them. The F_i and $\mathcal{F}_{ij}$ for the three surfaces shown in the figure are:

i-j	F_{ij}	$\mathcal{F}_{ij}$
1-2	0.393	0.139
1-3	0.235	0.152
2-3	0.594	0.249

Surface A_1 at temperature T_1 is the hotter trailing half of the ribbon, while A_2 at T_2 is the leading half. The temperature difference, $T_1 - T_2$, is due to the difference in the view factors F_{13} and F_{23}.

$$\frac{P_1}{A_1} = \sigma\mathcal{F}_{13}\left(T_1^4 - T_3^4\right) + \sigma\mathcal{F}_{12}\left(T_1^4 - T_2^4\right)$$

and (4)

$$\frac{P_2}{A_2} = \sigma\mathcal{F}_{23}\left(T_2^4 - T_3^4\right) - \sigma\mathcal{F}_{12}\left(T_1^4 - T_2^4\right)$$

The temperatures T_1 and T_2 are determined by equating the net power radiated away from each half of a ribbon to the rate of heating by the ions. The power balance is given by:

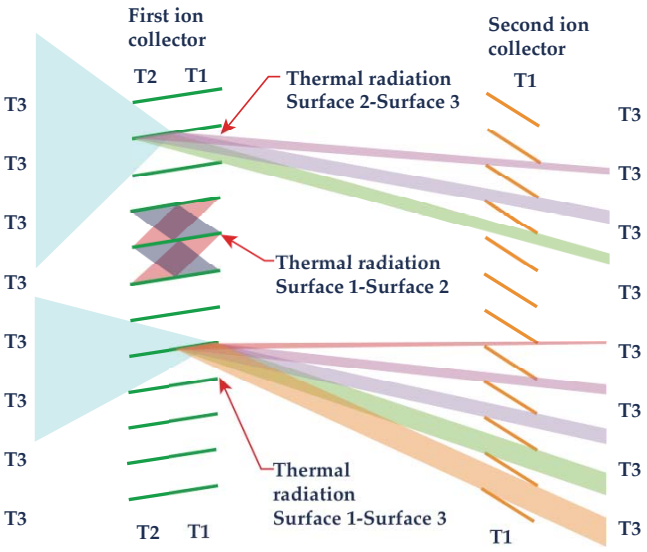

Figure 12 — Illustrating the view factors for radiation from each half of a ribbon to surfaces at other temperatures. $T_1 > T_2 > T_3$.

Here $P_1/A_1 = P_2/A_2 = 3$ W/cm² is the rate of heating of the ribbon by the ions, $\sigma = 5.68 \times 10^{-12}$ W cm^{-2}deg^{-4} is the Stefan-Boltzmann constant. When these two equations are solved, the result is:

$T_1 = 1110$°C, $T_2 = 1050$°C

A more accurate calculation would break each ribbon up into a larger number of isothermal pieces and would probably give a larger temperature gradient across the ribbon. The mean ribbon temperature would probably remain around 1080°C unless the emissivity or view factors to T_3 can be increased.

The temperature gradient across a ribbon presents a problem because of the differential expansion which could cause warping. We believe that warping can be prevented by tensioning the ribbons beyond the yield point.

It is apparent that adding a third collector between the two just discussed would require unacceptably high temperatures so we must abandon radiative cooling for more than two collectors.

Convective Heat Transfer

In order to increase the efficiency of the converter more collector stages can be added. For two collector stages radiative cooling can be considered, but for more than two a direct cooling method must be employed because the intermediate collectors would "see" mainly hot surfaces.

Figure 13 illustrates one possible way of cooling the collectors by forced convection. In the previously described case, the ribbons were only 0.13 mm thick. To provide room for coolant passages, the whole scale of the grid system is greatly increased while keeping the relative proportions more or less geometrically similar.

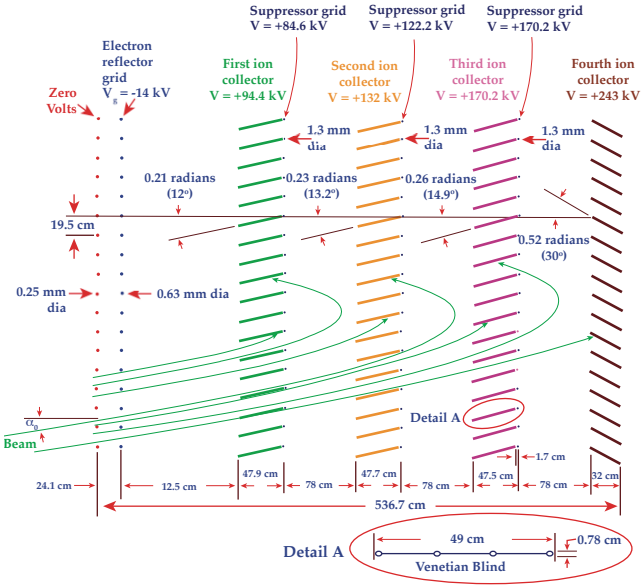

Figure 13 — Four-collector array with convective cooling. The spacings are as large as possible and set by space-charge considerations.

The ribbon shown here is constructed with a multiplicity of coolant passages. The coolant might be a high temperature liquid metal. Since the collectors are a high potential, the heat in the liquid metal could be transferred to helium in a heat exchanger at a high voltage. The helium then would be passed through insulated pipes to ground potential where the heat could then be converted to electricity in a conventional steam turbine. As an alternative,[22] helium at high pressure could be passed directly through the coolant passages. While the efficiency can be increased by using more collectors, because of the greater complications involved it is not clear without a detailed study that this would result in a lower $/kW price. Furthermore, it should be pointed out that the ability to replace the ribbons readily would be difficult to retain with convective cooling. In view of the probable radiation damage problem, this is an important advantage of the two-stage venetian blind scheme.

Applications to Toroidal Devices or Other Fusion Devices

In principle, the venetian blind direct converter could work on toroidal devices. The problems which we can anticipate are coupling the converter to the reactor diverter, effects due to different ion energy distributions, and different mean energies.

In Reference 5, there is shown a bumpy torus with a diverter connected to a direct converter. The direct converter could readily be connected to the type diverter used on the Model-C Stellarator. It is less easy to see

how to design a Tokomak whose diverter carries field lines out through the main coils; however in principle it seems possible.

Toroidal devices operating on the deuterium-tritium cycle tend to operate at mean energies of 10 to 40 keV. When the D-D-T- ^{3}He cycle is used, the mean energy is higher perhaps by 40 to 100 keV. If we try to use low energies (say about 100 keV mean energy) into the direct converter, the pumping problem will be difficult, although possibly tractable with some type of surface pumping. One uncertainty is how much ambipolar acceleration can be expected. Since it may be that the mean energy with the direct converter could be as much as the sum of the mean energy and electron energy inside the reactor, there could be up to a factor of almost 2 between mean energy inside and mean energy into the direct converter. If this is true, a 50-keV mean energy plasma could have 100-keV mean energy into the direct converter.

A more pessimistic possibility (which seems more likely at this moment) is that the Tokomak devices running on D-D-T-^{3}He cycle would radiate much of their energy away, largely negating the advantage in increasing the overall efficiency as discussed in Reference 5. The possibility of using this direct converter with tori fuel cycles having a large fraction of the energy release in the form of charged particles certainly needs investigating.

Application to Beam Energy Recovery

In the process of creating neutral beams, some ions will not be converted to neutrals or be trapped. The concept discussed in this paper could be applied to the recovery of these ion beams. Already, beams of 2 keV have been recovered with 95% efficiency.[23] It seems reasonable that the collection efficiency could be 98%; then, taking the other losses in Figure 11, we get a beam direct conversion efficiency of 89.4%. This application needs more study.

Cost Summary

The technique and basis used for estimating the cost is discussed in Reference 2. Essentially, it is the first-of-its-kind cost of building the device today. This was the technique used to estimate the 90-inch Livermore cyclotron, the Hilac, and the 88-inch cyclotron. The actual cost of a commercial device would of course have the benefit of considerable optimization and refinement. The cost summary is given in Table III and the detailed cost estimates are given in Table IV.

Table III — Cost Summary

Item	Dollars
Expander tank	$2,980K
Expander and neutron trap coils	$6,019K
Converter gate valve	$50K
Neutron trap shielding	$200K
Vacuum system	$3,000K
Grid system	$5,020K
Heat collection system	$1,060K
Electrical	$2,352K
Site preparation and utilities	$110K
Total cost for single unit	**$20,791K**
Cost for four units	$83,164K
Engineering	$12,475K
Contingency	$14,346K
Total facility (1973 dollars)	$109,985K

Table IV — Cost Estimates

Expander Tank		
Tank wall	1,360,000 kg	$1,490K
Rings	400,000 kg	$440K
Stiffeners	90,000 kg	$100K
Dished head	210,000 kg	$230K
Vacuum manifolds	170,000 kg	$190K
Grid system tank	260,000 kg	$290K
Support structure	220,000 kg	$240K
Total	2,710,000 kg	**$2,980K**

Note: above cost based on @$1.1/kg

Vacuum System	
122 cm diffusion pump (6)	
122 cm water-cooled baffle (1)	
Fore pump (4)	
Foreline valve and roughing valve (1)	
Diffusion pump oil (1)	
Instrumentation, interlocks (1)	
Installation (1)	
Total for 1 pump installation	$15K
Total for 200 pumps	**$3,000K**

Expander Coil and Neutron Trap Coil		
Superconducting coils, installed, neutron trap solenoid	1,040,000 kA meters @ $4/KA meter	$4,160K
Expander Coil	358,873 kA meters @$4/kA meter	$1,435K
Refrigeration	2.12 MW input power @$200/kW	$424K
Total		**$6,019K**

Converter / Trap	
Converter Gate Valve	$50K
Neutron Trap Shielding	$200K
Total	**$250K**

Grid System	
1440 niobium ribbons	$400K
1440 seals, spools, and drives, @$1,500	$2,160K
2160 wires (including seals, spools, drives) @$1,000 each	$2,160K
Insulators, shields	$300K
Total	**$5,020K**

Heat Collection System	
Water-cooled linear, 470,000 kg @$1.5/kg	$710K
Heat shields, 6,300 m² @$38/m²	$240K
Feed water system	$30K
Steam collection system	$80K
Total	**$1,060K**

Electrical Equipment	
Power supply, 13.8 kV, 50A, 690 kW	$77K
Power supply, 9.8 kV, 12.5A, 122.5 kW	$25K
Power supply, 180 kV, 0.5A 90 kW	$80K
75 MW inverter-rectifier assembly	$675K
75 MW transformer	$987K
75 MW Housing	$75K
Bushings	$2K
Cable	$50K
Harmonic filter	$50K
Power factor capacitor bank	$35K
Switchgear	$35K
Total	**$2,091K**

Miscellaneous	
Neutron trap power supply, 1.8 MW	$156K
Expander coil power supply, 240 KW	$40K
Control and instrumentation	$65K
Total	**$261K**

Site	
Site preparation	$30K
Foundations	$40K
Utilities	$20K
Inverter building	$20K
Total	**$110K**

Overall Costs	
Total cost for one unit	$20,791K
Cost for four (4) units	$83,164K
Engineering, 15%	$12,475K
Contingency, 15%	$14,346K
Total facility (1973 dollars)	**$109,985K**

Conclusions

We estimate the conversion efficiency of the venetian blind direct energy converter to be 59% for two collectors, 62% for three collectors, and 65% for four collectors operating at 150 keV injection energy.

The cost is estimated to be $28 M for an input power of 250 MW, or $110/kW. This can be compared to the fan-type direct converter which is estimated to operate at about 600 keV and 75% efficiency and cost $180/kW.

We believe that this preliminary engineering evaluation is sufficiently encouraging to warrant extensive further

work on the basic venetian blind scheme. The advantages of this scheme include:

- It lends itself to the use of a number of smaller units at a lower energy instead of one large one at a high energy so that one unit may be shut down for maintenance while the others are kept running.
- The cost in $/kW of direct converted power appears substantially lower.
- At least in the case where two collecting grids are used (and where radiative cooling may be used), the ribbons may be readily replaced if damaged by radiation.

The primary disadvantage is that the direct conversion efficiency is lower. It is apparent that the cooling problems are certainly difficult, but we feel they are by no means impossible. It is also clear that with a lower beam voltage the vacuum pumping problem soon becomes prohibitive.

Acknowledgments

We would like to thank Richard W. Werner for extensive discussions on the radiative and convective heat transfer problem and the radiation damage problem, Clyde E. Taylor for discussion on the superconductive and cryogenic system, and Phil Maslin for the illustrations.

We would also like to thank Richard F. Post, Bobby H. Smith, and T. Kenneth Fowler for their support of this work.

Publishing History

Received August 27, 1973, first published June 1974.

Reformatted and color illustrations added February 2009 by Mark Duncan.

References

[1] Richard F. Post; "Mirror systems: fuel cycles, loss reduction and energy recovery," in Proceedings of the British Nuclear Energy society Conference on Nuclear Fusion Reactors (Culham Laboratory, Culham, England, 1969) UKAEA (1970) 88-111.

[2] Bobby H. Smith, Richard H. Burleigh, Warren L. Dexter, Lewis L. Reginato; "An engineering study of the electrical design of a 1000-megawatt direct converter for mirror reactors," in Proceedings of the Texas Symposium on the Technology of Controlled Thermonuclear Fusion Experiments and the Engineering Aspects of Fusion Reactors, Austin, Texas, November 1972.

[3] Richard W. Werner, Gustav A. Carlson, Jack Hovingh, Joseph D. Lee, and M.A. Peterson; "Progress report #1 on the design considerations for a low power experimental mirror fusion reactor," in Proceedings of the Texas Symposium on the Technology of Controlled Thermonuclear Fusion Experiments and the Engineering Aspects of Fusion Reactors, Austin, Texas, November 1972.

[4] Ralph W. Moir and Clyde E. Taylor; "Magnets for open-ended fusion reactors," in Proceedings of the Texas Symposium on the Technology of Controlled Thermonuclear Fusion Experiments and the Engineering Aspects of Fusion Reactors, Austin, Texas, November 1972 (in press).

[5] Ralph W. Moir and William L. Barr; "'Venetian blind' direct energy converter for fusion reactors," Nuclear Fusion, 13, 35 (1973).

[6] Walt A. Perkins and J.C. Brown; "MAFCO — A magnetic field code for handling general current elements in three dimensions," Journal Applied Physics, 35, 3337 (1964).

[7] James H. Foote and Robert F. Freis; "Computer investigation of ion orbits in the Alice octupole and quadrupole magnetic fields," Controlled Thermonuclear Research Annual Report, July 1965 through June 1966, Lawrence Livermore Laboratory Report. UCRL-50002-66-1 (1966).

[8] P. C. Clemmow and J.P. Dougherty; "Electrodynamics of Particles and Plasmas," Addison-Wesley Publishing Co., Reading, MA (1969) pp. 90-99.

[9] Richard R. Smith; "Plasma Expander for Venetian Blind Direct Converters," Lawrence Livermore Laboratory Report UCRL-51373 (1973).

[10] Richard W. Werner; "Materials problems in direct conversion systems," in Proceedings of the AIME Spring Meeting on Design and Materials Problems in Thermonuclear Reactors, Boston, Massachusetts, May 8-9, 1972; also Richard W. Werner, Lawrence Livermore Laboratory, private communication (1973).

[11] Walter Bauer and G.J. Thomas; "Helium reemission and surface deformation in 316 stainless steel during -170°C to 700°C implantations," Journal Nuclear Materials.

[12] Walter H. Kohl; Handbook of Materials and Techniques for Vacuum Devices, Reinhold Publishing Company, New York (1967) pp. 252-259.

[13] Gustav A. Carlson; Lawrence Livermore Laboratory, private communication (19).

[14] Ralph W. Moir, William L. Barr, and Richard F. Post; "Experimental results on electrostatic stoppering," Physics Fluids, 14, 2531 (1971).

[15] Donald R. Sweetman et al; Neutral Injection Heating of Toroidal-Reactors, Culham Laboratory Report CLM-R112 (1971).

[16] William L. Barr; Lawrence Livermore Laboratory, private communication (1971).

[17] Archer H. Futch Jr.; J.P. Holdren; John Killeen and A.A. Mirin; "Multi-species Fokker-Planck calculations for D-T and D-^{3}He Mirror reactors Plasma Physics, 14, 211 (1972).

[18] The distributions in Figure 8 were calculated by A.H. Futch, Jr. for 100-keV injection and then scaled to 150-keV injection by multiplying the energy by 1.5 for use in this paper.

[19] Ralph W. Moir, William L. Barr, and Tom N. Haratani; Optimization of Collector Efficiency for Direct Energy Converters for Fusion Reactors, Lawrence Livermore Laboratory Report UCRL-51321 (1973).

[20] Richard W. Werner; Lawrence Livermore Laboratory private communication (1973).

[21] Warren H. Geidt; Principles of Engineering Heat Transfer (D. Van Nostrand Co., New York, 1957) pp. 252-259.

[22] Richard W. Werner; Lawrence Livermore Laboratory, private communication (1973).